C. R. Chimie 21 (2018) 696–703

Contents lists available at ScienceDirect

Comptes Rendus Chimie

www.sciencedirect.com

Full paper/Mémoire

Mn(III)-porphyrin/graphene oxide nanocomposite as an efficient catalyst for the aerobic oxidation of hydrocarbons

Saeed Rayati*, Saghar Rezaie, Fatemeh Nejabat

Department of Chemistry, K.N. Toosi University of Technology, P.O. Box 16315-1618, Tehran 15418, Iran

ARTICLE INFO

Article history:
Received 16 January 2018
Accepted 12 March 2018
Available online 14 April 2018

Keywords:
Metalloporphyrin
Graphene oxide
Heterogeneous catalysis
Oxidation reaction
Alkenes

ABSTRACT

In this study, manganese porphyrin was grafted on the surface of graphene oxide nanosheets via covalent bonding to produce a heterogeneous catalyst. The prepared nanocomposite was characterized using X-ray diffraction, UV–vis spectroscopy, scanning electron microscopy, Fourier transform infrared, and thermogravimetric analysis. Atomic absorption spectroscopy was also used to determine the amount of the loaded catalyst. The catalytic efficiency of the immobilized Mn-porphyrin was investigated for the aerobic oxidation of alkenes and saturated alkanes in acetone under mild reaction conditions. The prepared heterogenized catalyst displays superior catalytic performance as compared to the homogeneous catalyst. Moreover, the excellent turnover number (more than 31,767) achieved for the oxidation of styrene indicates the high longevity of the supported catalyst. The catalyst structure is preserved well after the oxidation reaction and is simply reused at least five times, without any significant loss of the catalytic efficiency.

1. Introduction

Catalytic oxidation of hydrocarbons in the liquid phase is a significant research area in synthetic organic chemistry due to the importance of the products being produced. These products are considered as valuable intermediates for the synthesis of various important substances, such as plasticizers, perfumes, and epoxy resins [1,2]. Since many years ago, metalloporphyrins as a useful model of cytochrome P-450 enzymes have held an important position in the catalytic oxidation reactions [3–6]. Recently, because of many benefits of heterogeneous catalysts like the ease of separation and reusability, metalloporphyrins are immobilized on the surface of various organic/inorganic substances for designing biomimetic heterogeneous catalysts [7–10]. According to the literature, different methods depending on the nature of solid supports and metalloporphyrins could be applied for the preparation of heterogenized metalloporphyrins. These methods mainly include encapsulation, adsorption, ionic interaction, axial coordination, and covalent bonding [11–14]. Graphene oxide (GO) with a large number of functional groups and a high surface area could be an excellent candidate as a solid support for the covalent immobilization of a variety of catalysts [15–17]. The use of green oxidants in the catalytic oxidation reactions remains an important challenge from the point of view of green chemistry [18,19]. Hydrogen peroxide as an inexpensive and environmentally friendly oxidant has been greatly used since long for catalytic oxidations of various organic substrates [20–22]. However, the instability of hydrogen peroxide in the catalytic reactions decreases its efficiency. This is considered as a major drawback in applying H_2O_2 as a green oxidant in the catalytic reactions. Molecular oxygen as a perfect oxidant with economically and environmentally friendly characters offers attractive prospects, especially in the industrial fields [23–25]. However, because of a poor product selectivity resulted for the catalytic oxidation reactions in which O_2 is used as an oxidant, many efforts have been focused on the

* Corresponding author.
E-mail address: rayati@kntu.ac.ir (S. Rayati).

https://doi.org/10.1016/j.crci.2018.03.003
1631-0748/

mechanistic study of these reactions. In addition, a great deal of attention has been paid to developing the selectivity and efficiency of the aforementioned reactions. As a continuation of our work on the oxidation of various organic substrates with green oxidants catalyzed by supported metalloporphyrins [8,14,26], herein, we report a reusable, highly efficient catalyst for aerobic oxidation of hydrocarbons under mild conditions.

2. Experimental section

2.1. Materials and characterization

Analytical grade chemicals were purchased from Merck and Fluka and used without further purification. Fourier transform infrared (FT-IR) spectra were obtained using potassium bromide pellets in the range 400–4000 cm^{-1} on an ABB Bomem FTLA 200-100 spectrophotometer. A Varian AA240 atomic absorption spectrometer was used for manganese determination. The UV–vis spectra were recorded using a Cam-Spec-M330 model. Scanning electron micrograph was taken using an EDf Oxford Mat 50 (Tescan vega3, lab6 model, magnification: 100,000). Gas chromatography experiments were performed by an Agilent 7890B instrument using an SAB-5 capillary column (phenyl methyl siloxane 30 m × 0.32 mm × 0.25 μm) and a flame ionization detector. The thermogravimetric analysis (TGA) and Differential Scanning Calorimetry (DSC) was carried out using Mettler Toledo (TGA-DSC), and X-ray diffraction (XRD) was recorded by Philips PW3710 at the angle range of 5–150° using Cu Kα radiation.

2.2. Preparation of Mn(THPP)OAc

5,10,15,20-Tetrakis(4-hydroxyphenyl)porphyrin (H_2THPP) was successfully prepared by the addition of 4-hydroxybenzaldehyde (1.1 g, 14.5 mmol) and pyrrole (0.62 mL, 14.46 mmol) to refluxing propionic acid as described by Adler et al. [27]. Mn(THPP)OAc was also prepared according to the procedure reported elsewhere [28].

2.3. Preparation of GO

GO was synthesized from natural graphite powder according to the modified Hummers' method [15,29]. Briefly, H_2SO_4 (360 mL) and H_3PO_4 (40 mL) were stirred and the graphite powder (3 g) was added to the acidic solution and sonicated for 30 min. Then, $KMnO_4$ (18 g) was gradually added to the mixture with stirring in an ice bath. After that, the mixture was stirred for 24 h at 50 °C to achieve GO. Subsequently, the mixture was diluted with deionized ice water (400 mL), and the oxidized product was treated with H_2O_2 (6 mL) to remove the residual permanganate ions. The GO product was collected by centrifuge and dried at 60 °C before further use.

2.4. Preparation of [Mn(THPP)OAc@GO]

Mn-porphyrin was covalently grafted to the GO nanosheets by the ester bond forming between the porphyrin hydroxyl groups and carboxylic acid groups of the GO. In this process, TBTU ((2-1*H*-benzotriazole-1-yl)-1,1,3,3-tetramethyluronium tetrafluoroborate) as a highly effective uronium salt is used as an activation agent for carboxylic acids to prepare esters in the presence of DIPEA (*N*,*N*-diisopropylethylamine) by the following procedure [30,31]: GO (1.5 g), TBTU (0.4 g), and DIPEA (0.3 g) were added to a solution of Mn(THPP)OAc (0.63 g) in DMF (70 mL), and the reaction mixture was vigorously stirred at room temperature for 48 h. The black solids were then collected by filtration, washed thoroughly with ethanol, and dried at 50 °C for about 24 h. Mn-porphyrin was immobilized onto the GO surface via the ester bond as reported in our previous study. Preparation of the catalyst has been schematically described in Scheme 1.

2.5. General procedure for aerobic oxidation of hydrocarbons

Oxidation of hydrocarbons (0.192 mmol) was initiated in a 5 mL test tube consisting of 1 mL acetone, 90 μL isobutyraldehyde (IBA) (0.960 mmol), 0.002 g catalyst, and 0.026 mmol imidazole (ImH) under the oxygen atmosphere, where the reaction mixture was stirred for 120 min at room temperature. The heterogenized catalyst was separated from the reaction media by a simple filtration. Gas chromatography was used to monitor the reaction progress, and the oxidation products were identified by comparison with the genuine samples.

3. Results and discussion

3.1. Characterization of the [Mn(THPP)OAc@GO] catalyst

Mn(THPP)OAc is anchored to the GO through covalent bonding between the hydroxyl group of the Mn-porphyrin and the carboxylic acid group of GO. The FT-IR spectra confirmed the covalent anchoring of Mn(THPP)OAc to the surface of GO (Fig. 1). An absorption band was observed at 856 cm^{-1} in the spectra of GO, which is related to the asymmetric epoxy on the GO surface [32]. Furthermore, the two peaks appeared at 1155 and 1596 cm^{-1} are respectively, related to the C–O and C=O stretching bands existing on the GO surface, and the broad peak observed at 3406 cm^{-1} corresponds to the –OH stretching band of GO. All these observations demonstrate that graphene was successfully converted to GO. In addition, the sharp peak

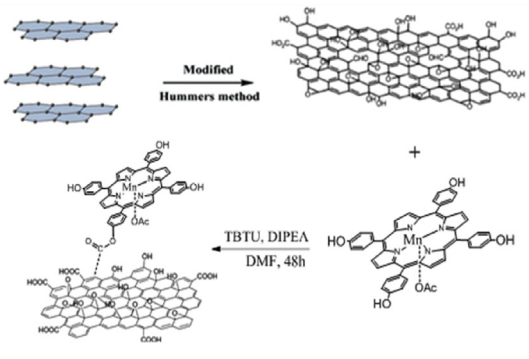

Scheme 1. Preparation of [Mn(THPP)OAc@GO].

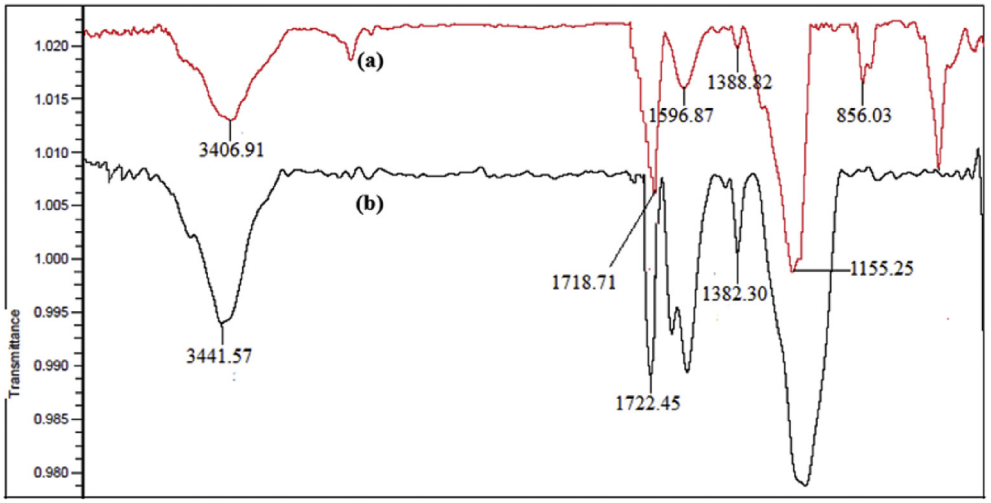

Fig. 1. FT-IR spectra of (a) GO and (b) [Mn(THPP)OAc@GO].

observed at 1718 cm^{-1}, which is related to the −COOH stretching band of the acidic groups of GO, was shifted to 1722 cm^{-1} as the metalloporphyrin was attached to GO-COOH. The C–O stretching band was also shifted from 1388 to 1382 cm^{-1}, indicating the formation of the ester bond between the metalloporphyrins and GO-nanosheets [15,32]. More details on the spectra can be found in Fig. 1.

The Mn content of the supported catalyst was determined by atomic absorption spectroscopy (AAS), and the result revealed that the amount of Mn-porphyrin in the catalyst is 750 μmol/g of the catalyst. The morphology and shape of [Mn(THPP)OAc@GO] were characterized by scanning electron microscopy (SEM). The SEM image of the prepared catalyst clearly exhibits randomly crumpled layer structures, indicating that the ordered layer structure in pristine graphite has been disrupted due to its oxidation [33]. It was also found that after the immobilization of Mn-porphyrin onto the GO surface, the nature of GO nanosheets remains unchanged (Fig. 2).

TGA of the GO and heterogeneous catalyst under N_2 gas atmosphere (100 mL/min) at a heating rate of 10 °C/min is illustrated in Fig. 3. Accordingly, the TGA thermogram of GO shows a weight loss at 100, 200, and 700 °C. The initial 16% weight loss at temperatures up to 120 °C was associated with the thermal desorption of water molecules adsorbed physically on the hydrophilic surface of the GO sheets (Fig. 3a). Moreover, thermal decomposition of the catalyst, which is accompanied by a significant weight loss of 35% at about 200 °C, is presumably due to the loss of the groups containing oxygen, such as hydroxyl, carboxyl, and epoxy groups before the complete oxidative decomposition of the graphitic substrate over 630–700 °C [34]. Owing to the fact that metalloporphyrins do not decompose below 300 °C under N_2 atmosphere, its incorporation onto the GO surface enhances the thermal stability of the nanocatalyst in comparison with pure GO (Fig. 3).

The UV–vis spectra of the dispersed GO and the GO attached to Mn(THPP)OAc are presented in Fig. 4. The spectrum of the GO dispersed in ethanol shows a strong absorption at about 219 nm and a broad absorption peak at 282 nm, originating from $\pi \rightarrow \pi^*$ and $n \rightarrow \pi^*$ transitions, respectively [35,36]. The characteristic Soret band of Mn-porphyrin at about 482 nm is clearly detectable in the spectrum of [Mn(THPP)OAc@GO] (with low intensity and observable red shift), confirming the presence of Mn(THPP)OAc on the surface of the GO nanosheets.

Additional verification of the successful hybridization of Mn(THPP)OAc with GO was provided by comparing the

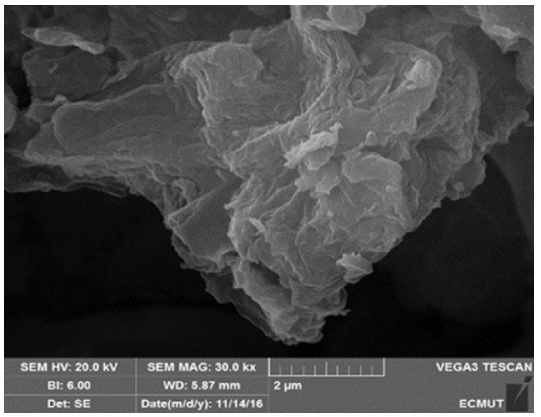

Fig. 2. SEM image of [Mn(THPP)OAc@GO].

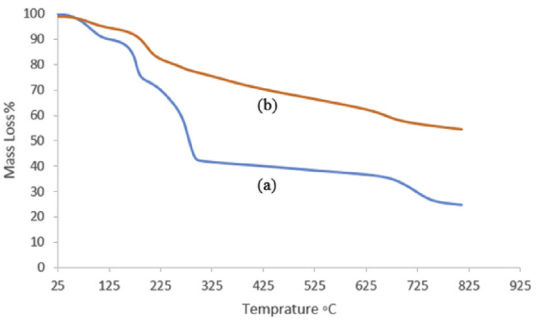

Fig. 3. The TGA thermograms of (a) GO and (b) [Mn(THPP)OAc@GO].

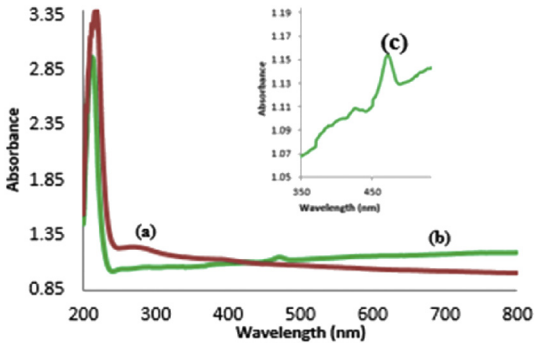

Fig. 4. UV–vis spectra of (a) GO and (b and c) [Mn(THPP)OAc@GO].

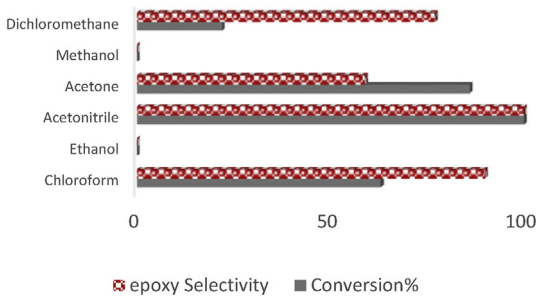

Fig. 6. Effect of various solvents on the oxidation of styrene with O_2 catalyzed by [Mn(THPP)OAc@GO]. The molar ratio of catalyst:ImH:styrene:IBA is 1:50:90:450. Reaction time: 90 min.

XRD patterns of pure GO and [Mn(THPP)OAc@GO] depicted in Fig. 5. Accordingly, in the XRD pattern of GO, the peak appeared at $2\theta = 18^\circ$ ($d_{001} = 4.81$ Å, 0.48 nm) corresponds to the layered structure of GO, and the presence of a characteristic diffraction peak for graphite at about $2\theta = 25^\circ$ ($d_{002} = 3.49$ Å, 0.34 nm) indicates that the graphite structure is largely preserved [37]. The XRD pattern of [Mn(THPP)OAc@GO] shows that the structure of the GO sheets remains unchanged after the immobilization of Mn-porphyrin onto the surface of GO. In addition, the distance between the GO layers does not change significantly ($d_{001} = 4.85$ Å, 4.85 nm and $d_{002} = 3.48$ Å, 0.348 nm).

3.2. Aerobic oxidation of hydrocarbons catalyzed by [Mn(THPP)OAc@GO]

The catalytic performance of [Mn(THPP)OAc@GO] in the heterogeneous oxidation of styrene as a model substrate with O_2 was investigated. To determine the best reaction condition, different parameters, such as the solvent nature, catalyst amount, and ImH/catalyst and IBA/catalyst molar ratios have been studied. The selection of the solvent could play a critical role in terms of achieving a high yield of product in the oxidation of alkenes. In this aspect, the aerobic oxidation of styrene was performed in various solvents, such as acetonitrile, ethanol, methanol, chloroform, dichloromethane, and acetone (Fig. 6).

It was observed that the catalytic efficiency of [Mn(THPP)OAc@GO] decreases in the order acetonitrile > acetone > chloroform > dichloromethane > methanol. Accordingly, the highest conversion was obtained in acetonitrile and acetone. Because acetone is cheaper and a fast evaporating solvent, it was chosen as the reaction solvent. Fig. 7 shows that the highest styrene conversion (98%) and the best selectivity were obtained after 2 h in acetone.

The catalyst concentration had a remarkable effect on the catalytic activity of [Mn(THPP)OAc@GO]. In the absence of metalloporphyrin and in the presence of pure GO, only 5% product was obtained. As it is seen from Table 1, an increase in the amount of catalyst from 0.001 to 0.002 g led to a significant increase in the conversion of styrene to the oxidation products. However, the use of 0.003 g of the catalyst caused a slight decrease in the efficiency of the oxidation reaction, and the further increase in the amount of catalyst was accompanied by a remarkable decrease in the conversion value. Although the comparison of entries 1 and 2 shows the presence of catalyst on the rate-limiting step of the oxidation reaction, the small decrease in the conversion value in the case of entry 3 and a remarkable decrease in the conversion yield of entry 4 cannot be explained on the basis of the know kinetics of the metalloporphyrin-catalyzed oxidation of organic compounds. The latter seems to originate from the decreased catalyst:IBA molar ratio from ca. 1:450 to 1:112 in the case of entries 1 and 4, respectively. This observation shows the great dependence of the oxidation reaction on the IBA concentration. Furthermore, the selectivity of reaction toward the styrene oxidation significantly increased in the case of the latter. This observation is also in accordance with the decreased efficiency of the formation of active

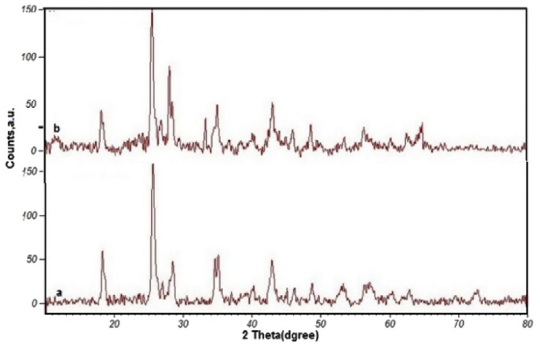

Fig. 5. XRD patterns of (a) GO and (b) [Mn(THPP)OAc@GO].

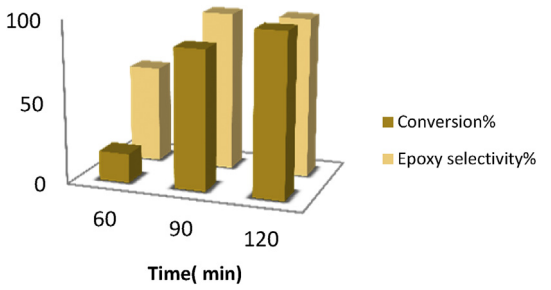

Fig. 7. Time effect on the oxidation of styrene with O_2 in acetonitrile catalyzed by [Mn(THPP)OAc@GO] at room temperature The molar ratio of [Mn(THPP)OAc@GO]:ImH:alkene:IBA is 1:50:90:450.

Table 1
The influence of the amount of catalyst on the oxidation of styrene with O_2 catalyzed by [Mn(THPP)OAc@GO] at room temperature.

Entry	Catalyst (g)	Conversion %[a]	Selectivity (epoxide) %
1	0.001	11	36
2	0.002	96	57
3	0.003	86	59
4	0.004	11	87

[a] The molar ratio of [Mn(THPP)OAc@GO]:ImH:styrene:IBA is *X*:50*X*:90:450. Reaction time: 2 h.

oxidant (manganese porphyrin peroxide intermediate) in the 1:112 molar ratio of the catalyst to IBA. It is noteworthy that the formation of overoxidation products, that is, carbonyl products occurs in the presence of higher concentrations of the peroxide intermediate [38].

The presence of a nitrogen-based component like ImH as a cocatalyst increases the catalytic activity of Mn-porphyrins in the oxidation reaction. The effect of ImH as an axial base on the catalytic oxidation of styrene with O_2 was examined, and the results are presented in Fig. 8. The addition of ImH up to 50:1 ratio relative to the catalyst made an increase in the conversion of reaction, whereas beyond this ratio, a significant decrease was observed in the yield of product. This may be due to the formation of inactive six-coordinate species, that is, $Mn(THPP)(ImH)_2$ [39].

The aerobic oxidation of olefins at room temperature needs a reducing agent, such as IBA for the reduction of dioxygen at the beginning of the reaction [19,40]. The effect of an IBA:styrene molar ratio on the catalytic activity of [Mn(THPP)OAc@GO] was also studied. The results confirmed that the presence of IBA is essential for the activation of dioxygen, and the highest conversion was achieved in the presence of a 5:1 (IBA:styrene) molar ratio after 2 h (Table 2). Furthermore, the examination of the temperature effect on the catalytic oxidation reaction revealed that with increasing the reaction temperature from 25 to 45 °C, the reaction time decreases to 90 min. Although at higher temperatures, the catalytic oxidation will finish in a shorter time as compared to lower temperatures, the selectivity to the epoxide product decreases as temperature increases.

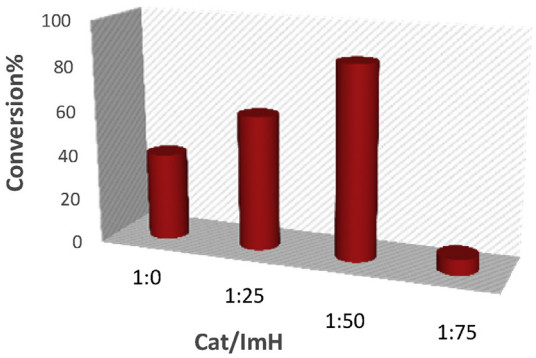

Fig. 8. Effect of catalyst:ImH molar ratios on the oxidation of styrene with O_2 in acetone catalyzed by [Mn(THPP)OAc@GO] at room temperature. The molar ratio of catalyst:ImH:alkene:IBA is 1:*X*:90:630.

Table 2
Influence of an IBA molar ratio on the oxidation of styrene with O_2 in acetone catalyzed by [Mn(THPP)OAc@GO].

Entry	IBA/styrene	Temperature (°C)	Conversion%[a]	Selectivity (epoxide) %
1	0	25	0	–
2	2	25	13	46
3	3	25	32	59
4	5	25	98	57
5	5	5	6	100
6	5	25[b]	83	100
7	5	45[b]	100	35

[a] The molar ratio of catalyst:ImH:styrene:IBA is (1:50:90:*X*). Reaction time: 2 h.
[b] Reaction time: 90 min.

3.3. Heterogeneous oxidation of different hydrocarbons

To evaluate the applicability of the proposed catalytic system, a series of olefins and alkanes were subjected to the reaction in the presence of [Mn(THPP)OAc@GO] under the optimized conditions, and the results obtained are given in Table 3. Accordingly, all the substrates are oxidized in the presence of a catalytic amount of supported Mn-porphyrin under mild conditions. In the case of styrene, α-methylstyrene, 4-methylstyrene, cyclooctene, 1-octene, *trans*-stilbene, and the corresponding epoxide were produced as major products (Table 3, entries 1–8). In the oxidation of cyclohexene, 45% epoxy, 15% cyclohexen-2-one, and 17% cyclohexen-2-ole were obtained. In the oxidation of indane, 17% indanone and 2% 1-indanole were detected as products, and adamantane was oxidized to 1-adamantanol in 92% yield. It should be noted that a less activity was observed for 1-octene (11%) as a linear terminal olefin with lower reactivity (Table 3).

3.4. Catalyst reuse and stability

The stability and reusability of a heterogeneous catalyst are two most important factors in the catalytic systems, especially in industrial and commercial applications. The prepared catalyst can be separated easily and reused several times. For each of the repeated reactions, after the completion of the reaction, the solid catalyst was removed by centrifugation for about 15 min, washed with acetone and methanol (2 × 1 mL), dried at 50 °C for 20 h, and used for the next run. Fig. 9 shows the reusability of [Mn(THPP)OAc@GO] for the aerobic oxidation of styrene under the optimized conditions, which clearly describes the stability and efficiency of Mn(THPP)OAc after deposition on the GO surface. Furthermore, to estimate the longevity of the heterogeneous catalytic system, total turnover number has been evaluated. The catalyst exhibits an excellent activity for the oxidation of styrene in the acetone solution under mild conditions (Cat.:styrene:IBA is 1:35,000:90,000) with a turnover number of 31,767 after 4 days, which is considered to be a remarkable value for a heterogeneous catalytic system.

To evaluate the catalytic efficiency and reusability of [Mn(THPP)OAc@GO] for epoxidation with molecular oxygen, the obtained results were compared with some

Table 3
Oxidation of various hydrocarbons using molecular oxygen and IBA, catalyzed by [Mn(THPP)OAc@GO] in the presence of ImH in acetone room temperature.

Entry	Substrate	Product	Conversion%[a]	Selectivity%[b]
1		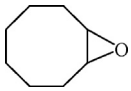	78	100
2	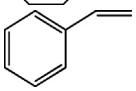	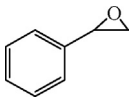	100	85
3		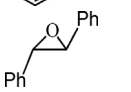	88	80
4	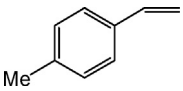	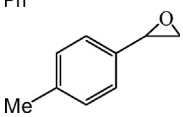	91	100
5	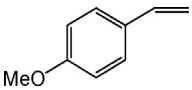	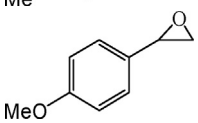	100	91
6	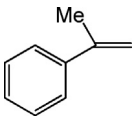	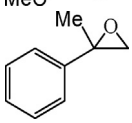	100	100
7	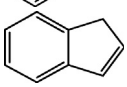	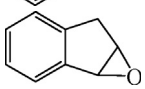	89	84
8	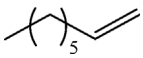	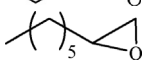	11	100
9	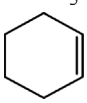	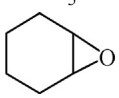	77	58
10	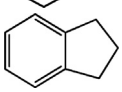	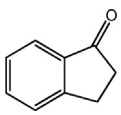	19	89
11		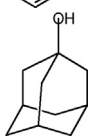	92	100

[a] The molar ratio of catalyst:ImH:styrene:IBA is (1:50:90:450). Reaction time: 2 h.
[b] The GC yields (%) for oxidation of alkene are measured relative to the starting substrate.

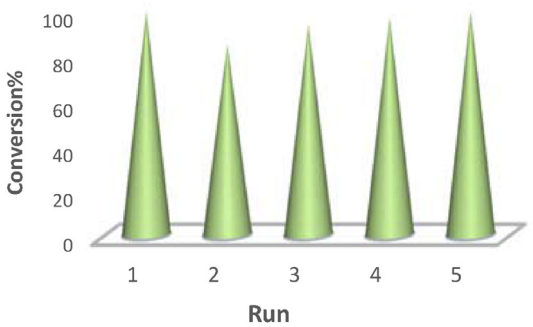

Fig. 9. The recovery and reuse of [Mn(THPP)OAc@GO] on the oxidation of styrene.

previously reported data, which clearly shows the advantages of the present method in terms of catalytic activity and reusability (Table 4).

4. Proposed mechanism

Various methods have been reported for the activation of molecular oxygen in the catalytic oxidation reactions, and aldehyde is a common coreductant in the aerobic oxidations [19]. According to the literature, the oxidation of organic substrates with molecular oxygen and aldehyde can be assumed a free radical mechanism and two parallel pathways could be possible in the presence of metal complexes (Scheme 2) [40,44,45]. Acyl peroxy radical (Scheme 2, II) is the most active species in this catalytic cycle, which can be generated from acyl radical (Scheme 2, I) and

Table 4
A comparison of the presented catalytic system with some previously reported cases for epoxidation with green oxidants in the presence of porphyrin-based catalysts.

No.	Catalyst	Oxidant	No. of runs	Conversion% (first run–last run)	Reference
1	Mn(Porph)-MR	H_2O_2	5	92–57	[21]
2	Fe(THPP)Cl@MWCNT	H_2O_2	5	80–36	[26]
3	Mn(THPP)OAc@MWCNT	H_2O_2/Ac_2O	5	100–97	[8]
4	Mn(TPP)OAc/MCM-41	UHP/HOAc	3	95–38	[14]
5	MNP@SiO_2[Mn(III) TDCPP-NH_2]	O_2/IBA	4	99–96	[41]
6	MOF-525-Mn	O_2/IBA	6	83–83	[42]
7	Fe_3O_4/tart/Mn(TCPP)Cl	O_2/IBA	6	73–62	[40]
8	Fe(THPP)Cl@MWCNT	O_2/IBA	5	100–78	[43]
9	Mn(THPP)OAc@GO	O_2/IBA	5	100–100	This work

molecular oxygen. Acyl peroxy radical directly promotes the epoxidation of olefins and generates the acyl radical for the next cycle or for acting with another aldehyde to produce peroxycarboxylic acid (Scheme 2, III). Furthermore, the high-valent Mn–oxo species (Scheme 2, IV) as usual active species in the catalytic cycles of metalloporphyrin can be produced in the presence of peroxycarboxylic acid and metalloporphyrin [45,46]. Finally, the high-valent Mn–oxo as unstable intermediate reacts rapidly with olefin to produce epoxy and carboxylic acid as a byproduct of the reaction process [19].

According to our previous studies [6,10,47,48], Mn(III) and/or Fe(III) porphyrin hydroperoxo and high-valent Mn–oxo species are the main active oxidants involved in the oxidation of organic compounds with hydrogen peroxide catalyzed by manganese(III) or iron(III) porphyrins. In addition, in the presence of molecular oxygen and IBA as the reducing agent, the same species seem to be the active oxidants (Scheme 2). However, due to the lack of free hydrogen peroxide molecules in this catalytic system, the side reactions that occur in the presence of radical species like hydroxyl radical formed by hydrogen peroxide are probably prevented. The latter can decrease the epoxide selectivity of the oxidation reaction. Moreover, the radical species can initiate an autoxidation pathway [49] for the oxidation reaction. It is noteworthy that in contrast to organic peracids, aqueous hydrogen peroxide needs a metal complex to be activated and perform the oxidation reactions [49]. Therefore, hydrogen peroxide cannot directly oxidize the organic substrates with lower reactivity, such as olefins.

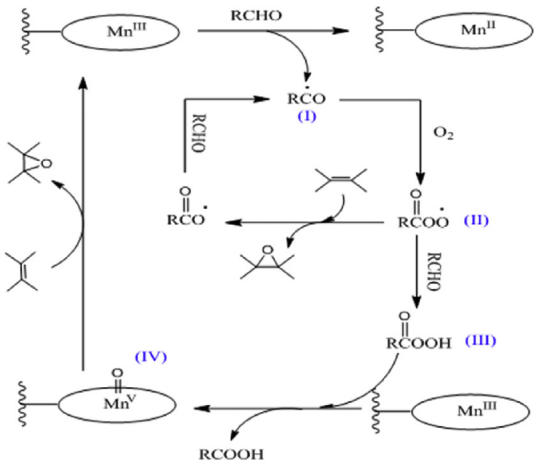

Scheme 2. Proposed catalytic cycle.

5. Conclusions

To sum up, Mn(THPP)OAc was grafted on the GO surface to provide an effective catalytic system for oxidizing various alkenes and alkanes to the corresponding oxidation products like epoxy and alcohols. The present method offers several advantages, such as the high yield of products, short reaction time, mild conditions, simple workup procedure, and reusability of the catalyst without a significant loss in conversion and selectivity.

Acknowledgments

We gratefully acknowledge the practical support of this study by K.N. Toosi University of Technology.

References

[1] M. Beller, C. Bolm, Transition Metals for Fine Chemicals and Organic Synthesis, vol. 2, Wiley, Weinheim, Germany, 1998, pp. 261–267.
[2] A. Zarrinjahan, M. Moghadam, V. Mirkhani, S. Tangestaninejad, I. Mohammadpoor-Baltork, J. Iran. Chem. Soc. 13 (2016) 1509–1516.
[3] A. Rezaeifard, M. Jafarpour, Catal. Sci. Technol. 4 (2014) 1960–1969.
[4] S. Zakavi, Z. Kayhomayoon, S. Rayati, J. Iran. Chem. Soc. 12 (2015) 863–872.
[5] S. Rayati, F. Nejabat, S. Zakavi, Inorg. Chem. Commun. 40 (2014) 82–86.
[6] S. Rayati, Z. Sheybanifard, C. R. Chimie 19 (2016) 371–380.
[7] H. Zhang, Y. Sun, K. Ye, P. Zhang, Y. Wang, J. Mater.Chem. 15 (2005) 3181–3186.
[8] S. Rayati, E. Bohloulbandi, C. R. Chimie 17 (2014) 62–68.
[9] X. Zhou, H. Ji, J. Porphyr. Phthalocyanines 16 (2012) 1033–1039.
[10] S. Rayati, F. Nejabat, C. R. Chimie 20 (2017) 967–974.
[11] P. Zucca, C.M.B. Neves, M.M.Q. Simões, G.P.M.S. Neves, G. Cocco, E. Sanjust, Molecules 21 (2016) 964–1004.
[12] S. Nakagaki, K.M. Mantovani, G.S. Machado, K. Aparecida, D. De Freitas, F. Wypych, Molecules 21 (2016) 291–315.

[13] C.F. Pereira, M.M.Q. Simões, J.P.C. Tomé, F.A.A. Paz, Molecules 21 (2016) 1348–1367.
[14] S. Rayati, S.E. Ruzbahani, F. Nejabat, Macroheterocycles 10 (2017) 57–61.
[15] W.S. Hummers, R.E. Offeman, J. Am. Chem. Soc. 80 (1958) 1339.
[16] A. Zarnegaryan, M. Moghadam, S. Tangestaninejad, V. Mirkhani, I. Mohammdpoor-Baltork, New J. Chem. 40 (2016) 2280–2286.
[17] Y. Rongbing, S. Zhang, Y. Luo, R. Bai, J. Zhou, H. Song, New J. Chem. 39 (2015) 5096–5099.
[18] M. Sahoo, K.M. Parida, Appl. Catal. A 460 (2013) 36–45.
[19] A. Mukherjee, in: H.B. Ji, X.T. Zhou (Eds.), Biomimetic Based Applications, In Tech, India, 2011.
[20] K. Kaczorowska, Z. Kolarska, K. Mitka, P. Kowalski, Tetrahedron 61 (2005) 8315–8327.
[21] R. De Paula, I.C.M.S. Santos, M.M.Q. Simões, M.G.P.M.S. Neves, J.A.S. Cavaleiro, J. Mol. Catal. A Gen. 404 (2015) 156–166.
[22] P. Zucca, G. Cocco, M. Pintus, A. Rescigno, E. Sanjust, J. Chem. 2013 (2013) 1–7.
[23] L. Zhifang, S. Wu, H. Ding, H. Lu, J. Liu, Q. Huo, Q. Kan, New J. Chem. 37 (2013) 4220–4229.
[24] H. Tanaka, H. Nishikawa, T. Uchida, T. Katsuki, J. Am. Chem. Soc. 132 (2010) 12034–12041.
[25] R. Rahimi, E. Gholamrezapor, M.R. Naimi-jamal, Inorg. Chem. Commun. 14 (2011) 1561–1568.
[26] S. Rayati, Z. Sheybanifard, J. Porphyr. Phthalocyanines 19 (2015) 622–630.
[27] A.D. Adler, F.R. Longo, W. Shergalis, J. Am. Chem. Soc. 86 (1964) 3145–3149.
[28] A.D. Adler, F.R. Longo, F. Kampas, J. Kim, J. Inorg. Nucl. Chem. 32 (1970) 2443–2445.
[29] L. Wu, L. Yu, X. Ding, P. Li, X.D. Xiaomei Chen, H. Zhou, Y. Bai, J. Ding, Food Chem. 217 (2017) 320–325.
[30] S. Rayati, P. Jafarzadeh, S. Zakavi, Inorg. Chem. Commun. 29 (2013) 40–44.
[31] S. Balalaie, M. Mahdodust, R.E. Eshghi-Najafabadi, Chin. J. Chem. 26 (2008) 1141–1144.
[32] D.L. Pavia, G.M. Lampman, G.S. Kriz, J.A. Vyan, Introduction to Spectroscopy, Cengage Learning, 2008.
[33] H. Wang, Y.H. Hu, Ind. Eng. Chem. Res. 50 (2011) 6132–6137.
[34] A.B. Bourlinos, D. Gournis, D. Petridis, T. Szabo, A. Szeri, I. Dekany, Langmuir 19 (2003) 6050–6055.
[35] W. Zheng, R. Tan, L. Zhao, Y. Chen, C. Xiong, D. Yin, RSC Adv. 4 (2016) 17073–17079.
[36] V.H. Pham, H.D. Pham, T.T. Dang, S.H. Hur, E.J. Kim, B.S. Kong, S. Kim, J.S. Chung, J. Mater. Chem. 22 (2012) 10530–10536.
[37] X.Q. Zhang, Y.Y. Feng, D. Huang, Y. Li, W. Feng, Carbon 48 (2010) 3236–3241.
[38] S. Zakavi, A.G. Mojarrad, S. Rayati, J. Mol. Catal. A Chem. 363–364 (2012) 153–158.
[39] D. Mohajer, G. Karimipour, M. Bagherzadeh, New J. Chem. 28 (2004) 740–747.
[40] A. Farokhi, M. Hosseini-Monfared, New J. Chem. 40 (2016) 5032–5035.
[41] J.W. Brown, Q.T. Nguyen, T. Otto, N.N. Jarenwattananon, S. Glöggler, L. Bouchard, Catal. Commun. 59 (2015) 50–54.
[42] L.D. Dias, R.M.B. Carrilho, C.A. Henriques, G. Piccirillo, A. Fernandes, M.M. Rossi, M.F. Ribeiro, M.J.F. Calvete, J. Porphyr. Phthalocyanines 22 (2018) 1–11.
[43] M.J. Beier, W. Kleist, M.T. Wharmby, R. Kissner, B. Kimmerle, P.A. Wright, J.D. Grunwaldt, A. Baiker, Chem. Eur. J. 18 (2012) 887–898.
[44] S. Rayati, F. Nejabat, New J. Chem. 41 (2017) 7987–7991.
[45] I. Tabushi, A. Yazaki, J. Am. Chem. Soc. 103 (1981) 7371–7373.
[46] Y. Tsuda, K. Takahashi, T. Yamaguchi, S. Matsui, T. Komura, J. Mol. Catal. 130 (1998) 285–295.
[47] S. Rayati, Z. Sheybanifard, M.M. Amini, A. Aliakbari, J. Mol. Catal. A 423 (2016) 105–113.
[48] S. Rayati, F. Nejabat, Polyhedron 104 (2016) 52–57.
[49] R.A. Sheldon, J.K. Kochi, Metal-catalyzed Oxidations of Organic Compound, Academic Press, Inc, London, 1981.